XII International Conference on Computational Plasticity. Fundamentals and Applications
COMPLAS XII
E. Oñate, D.R.J. Owen, D. Peric and B. Suárez (Eds)

HOMOGENIZED MODEL FOR HERRINGBONE BOND MASONRY: LINEAR ELASTIC AND LIMIT ANALYSIS

GABRIELE MILANI*

* Department of Architecture, Built Environment and Construction Engineering ABC
Politecnico di Milano
Piazza Leonardo da Vinci 32, 20133 Milan, Italy
e-mail: gabriele.milani@polimi.it

Key words: Masonry, Homogenization, Limit analysis, Elasticity.
Abstract. A kinematic procedure to obtain in-plane elastic moduli and macroscopic masonry strength domains in the case of herringbone masonry is presented. The model is constituted by two central bricks interacting with their neighbors by means of either elastic or rigid-plastic interfaces with friction, representing mortar joints.
A sub-class of possible elementary deformations is a-priori chosen to describe joints cracking under in- plane loads. Suitable internal macroscopic actions are applied on the Representative Element of Volume REV and the power expended within the 3D bricks assemblage is equated to that expended in the macroscopic 2D Cauchy continuum. The elastic and limit analysis problem at a cell level are solved by means of a quadratic and linear programming approach, respectively.
When dealing with the limit analysis approach, several computations are performed investigating the role played by (1) the direction of the load with respect to herringbone bond pattern inclination and (2) masonry texture.

1 INTRODUCTION

Masonry modelling may be performed by means of both micromechanical and macroscopic approaches or adopting homogenization techniques [1]-[4], based either on averaging procedures or simplified models of direct identification (compatible or equilibrated). In this framework, different constitutive masonry models have been proposed in the literature. Generally speaking, the assumptions to make for a correct macroscopic characterization are strongly connected to masonry geometry (texture), as well as bricks and mortar mechanical behavior. In the literature, blocks have been modeled as rigid [1], deformable with damage [2], whereas for mortar either a full continuum representation was adopted [2][4] or the interface concept was preferred to improve computational efficiency [5]-[7].

Many efforts have been expended to analyse regular arrangements with blocks disposed in running bond, however, at present, research appears still somewhat fragmented when dealing with herringbone bond masonry, even if some preliminary studies have been very recently proposed (e.g. [8]).

The present paper aims for better insight into the elastic and limit state behavior of herringbone bond masonry in-plane loaded by means of a novel compatible identification

approach. In particular, the 3D continuum is modeled by means of a 2D approach, where the contemporary presence of bricks and mortar is accounted for by means of a rigid internal microstructure.

In the model, blocks are supposed rigid and joints are reduced to interfaces, in order to obtain a realistic prediction of the actual behavior of herringbone bond masonry in the linear elastic range and near collapse (ultimate behavior). Then, a numerical procedure of identification between the 3D discrete Lagrangian system and a continuum equivalent model is imposed in terms of power dissipated in the 3D discrete model and in the continuum. A Cauchy continuum is adopted under either the assumption of elastic and rigid-plastic (limit analysis) behavior for mortar joints reduced to interfaces.

When dealing with the elastic case, since deformation can take place only at the interface between bricks when bricks are assumed rigid, a simple quadratic programming problem in few variables is obtained to evaluate homogenized elastic moduli.

The extension to rigid-plastic materials requires the combination of homogenization concepts and classic limit analysis theorems. Following the general procedure adopted by the author for running [9] and English bond [10] textures and using the compatible model utilized for deducing homogenized elastic moduli, herringbone masonry is studied at failure within the classic hypothesis holding for limit analysis to provide upper bound estimates of the homogenized masonry failure surfaces.

Several numerical examples are analyzed, to evaluate the sensitivity of the results to (1) direction of the load with respect to herringbone bond inclination and (2) masonry texture.

2 COMPATIBLE IDENTIFICATION MODEL

A masonry wall constituted by blocks arranged in herringbone bond is considered, as schematically sketched in Figure 1. The block dimensions are *a*, *b* (height and length) and *t* (thickness).

The 3D assemblage of blocks (heterogeneous model) under consideration occupies a domain $\Omega\times]-\frac{t}{2},\frac{t}{2}[$ where Ω is the middle surface of the equivalent 2D plate and shell model and t is its thickness, that coincides, in this case, with the thickness of a single block.

The arrangement is periodic in the space and the Representative Elementary Volume (REV) is chosen in order to contain all the information necessary to geometrically describe the entire masonry wall.

The module is denoted by $Y=\omega\times]-\frac{t}{2},\frac{t}{2}[$, where $Y\subset \Re^3$ and $\omega\subset\Omega$. The boundary of Y is denoted by $\partial Y=\partial Y_l\cup\partial Y_3^+\cup\partial Y_3^-$, $\partial Y_3^{\pm}=\omega\times\pm\frac{t}{2}$.

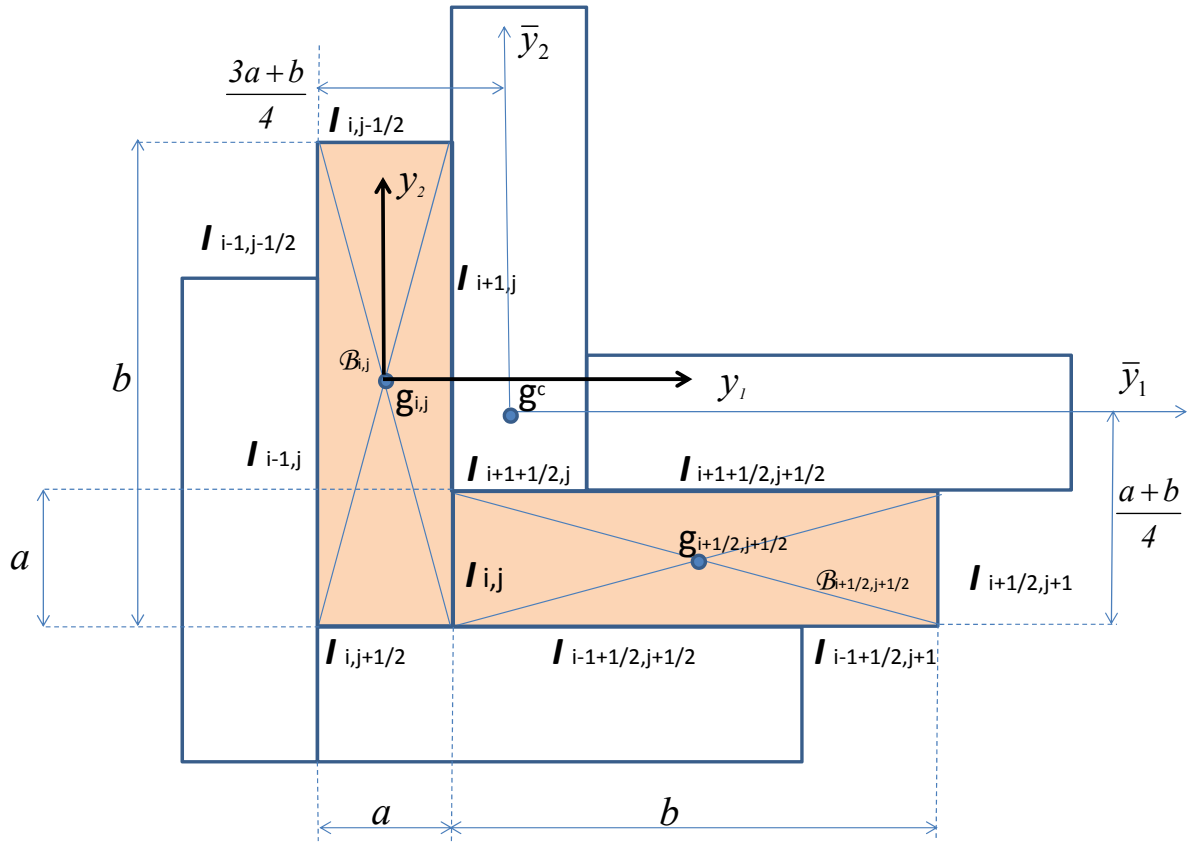

Figure 1: REV assumed in the simulations for herringbone bond masonry.

According to Figure 1, the position of a block centroid is univocally characterized by two indices. In particular, a block with its b length disposed parallel to the vertical direction is defined by the indices (i, j), while a block with its b length disposed parallel to the horizontal direction is defined by the indices $(i+1/2, j+1/2)$. In this way, the position of all blocks may be defined according to the representation of Figure 1.
Hence, the $\mathbf{g}_{i,j}$ centroid of the block $B_{i,j}$ is defined as:

$$\mathbf{g}_{i,j} = \begin{Bmatrix} (i\boldsymbol{\alpha}_1 + j\boldsymbol{\alpha}_2)\mathbf{e}_1 \\ (i\boldsymbol{\alpha}_1 + j\boldsymbol{\alpha}_2)\mathbf{e}_2 \end{Bmatrix} = \begin{Bmatrix} ia + jb \\ ia - jb \end{Bmatrix} \tag{1}$$

whereas the $\mathbf{g}_{i+\frac{1}{2},j+\frac{1}{2}}$ centroid of the block $B_{i+\frac{1}{2},j+\frac{1}{2}}$ is defined as:

$$\mathbf{g}_{i+\frac{1}{2},j+\frac{1}{2}} = \begin{Bmatrix} \left(\left(i+\frac{1}{2}\right)\boldsymbol{\alpha}_1 + \left(j+\frac{1}{2}\right)\boldsymbol{\alpha}_2\right)\mathbf{e}_1 \\ \left(\left(i+\frac{1}{2}\right)\boldsymbol{\alpha}_1 + \left(j+\frac{1}{2}\right)\boldsymbol{\alpha}_2\right)\mathbf{e}_2 \end{Bmatrix} = \begin{Bmatrix} \left(i+\frac{1}{2}\right)a + \left(j+\frac{1}{2}\right)b \\ \left(i+\frac{1}{2}\right)a - \left(j+\frac{1}{2}\right)b \end{Bmatrix} \tag{2}$$

Thus, the basic pattern is represented by two blocks. The pattern exhibits 1 internal interface and 10 external interfaces, 5 for the block $B_{i,j}$ and 5 for the block $B_{i+\frac{1}{2},j+\frac{1}{2}}$.

The symbol $\mathrm{I}_{\mathrm{i,j}}$ in Figure 1 indicates the internal interface between $B_{i,j}$ and $B_{i+\frac{1}{2},j+\frac{1}{2}}$, the symbol $\mathrm{I}_{\mathrm{i+k_1,j+k_2}}$ indicates the external interfaces of $B_{i,j}$ block and the symbol $\mathrm{I}_{\mathrm{i+\frac{1}{2}+k_1,j+\frac{1}{2}+k_2}}$ the external interfaces of $B_{i+\frac{1}{2},j+\frac{1}{2}}$ block.

The compatible equivalent model bases on a correspondence between equivalent class of motions in the discrete blocks system and a plane continuous model.

A portion of a $\mathcal{P}$ masonry panel (continuous model) with the same dimensions of the REV (discrete block system model) is considered, see Figure 2. This portion is chosen so that its center $\mathbf{g}^{\mathrm{c}}$ coincides with the center of the REV. A portion of panel $\mathcal{H}$, with the same edge is considered, so that the $\mathbf{x}$ point of $\mathcal{H}$ coincides with $\mathbf{g}^{\mathrm{c}}$ (this is the center of pattern represented in Figure 1).

In the discrete system, the motion of a generic couple of blocks $B_{i,j}$ and $B_{i+\frac{1}{2},j+\frac{1}{2}}$ may be described as a function of their center velocity $\dot{\mathbf{w}}^{i,j}$, $\dot{\mathbf{w}}^{i+\frac{1}{2},j+\frac{1}{2}}$ and their angular velocity $\boldsymbol{\Omega}^{i,j}$, $\boldsymbol{\Omega}^{i+\frac{1}{2},j+\frac{1}{2}}$. In what follows, for the sake of simplicity, the generic interface (either internal or external) will be indicated with I symbol. Let $\mathbf{p}$ be the center of the I interface between $B_{i,j}$ and $B_{i+\frac{1}{2},j+\frac{1}{2}}$. The velocity of the material points $\mathbf{x}$ of $B_{i,j}$ and $B_{i+\frac{1}{2},j+\frac{1}{2}}$ in contact in a position $\boldsymbol{\xi} \in \mathrm{I}$, may be written as:

$$\begin{aligned}
&\dot{\mathbf{w}}^{i,j}(\mathbf{x}) = \dot{\mathbf{w}}^{i,j}(\mathbf{p}) + \boldsymbol{\Omega}^{i,j}(\boldsymbol{\xi} - \mathbf{p}) \\
&\dot{\mathbf{w}}^{i+\frac{1}{2},j+\frac{1}{2}}(\mathbf{x}) = \dot{\mathbf{w}}^{i+\frac{1}{2},j+\frac{1}{2}}(\mathbf{p}) + \boldsymbol{\Omega}^{i+\frac{1}{2},j+\frac{1}{2}}(\boldsymbol{\xi} - \mathbf{p})
\end{aligned} \tag{3}$$

The strain rate may be written as function of jump of the velocity field $\dot{\mathbf{w}}(\boldsymbol{\xi})$ between $B_{i,j}$ and $B_{i+\frac{1}{2},j+\frac{1}{2}}$. in a point $\boldsymbol{\xi} \in \mathrm{I}$:

$$\begin{aligned}
&\left\lfloor \dot{\mathbf{w}}(\boldsymbol{\xi}) \right\rfloor = \dot{\mathbf{w}}^{i+\frac{1}{2},j+\frac{1}{2}}(\boldsymbol{\xi}) - \dot{\mathbf{w}}^{i,j}(\boldsymbol{\xi}) = \\
&= \dot{\mathbf{w}}^{i+\frac{1}{2},j+\frac{1}{2}}(\mathbf{p}) - \dot{\mathbf{w}}^{i,j}(\mathbf{p}) + \boldsymbol{\Omega}^{i+\frac{1}{2},j+\frac{1}{2}}(\boldsymbol{\xi} - \mathbf{p}) - \boldsymbol{\Omega}^{i,j}(\boldsymbol{\xi} - \mathbf{p}) = \\
&= \dot{\mathbf{w}}_p + \boldsymbol{\Omega}_p(\boldsymbol{\xi} - \mathbf{p})
\end{aligned} \tag{4}$$

where: $\dot{\mathbf{w}}_p = \dot{\mathbf{w}}^{i+\frac{1}{2},j+\frac{1}{2}}(\mathbf{p}) - \dot{\mathbf{w}}^{i,j}(\mathbf{p})$ and $\boldsymbol{\Omega}_p = \boldsymbol{\Omega}^{i+\frac{1}{2},j+\frac{1}{2}} - \boldsymbol{\Omega}^{i,j}$.

For the homogenized model, reference is made to a bi-dimensional Cauchy continuum identified by its middle plane $\mathcal{S}$ of normal $\mathbf{e}_3$ (Figure 2).

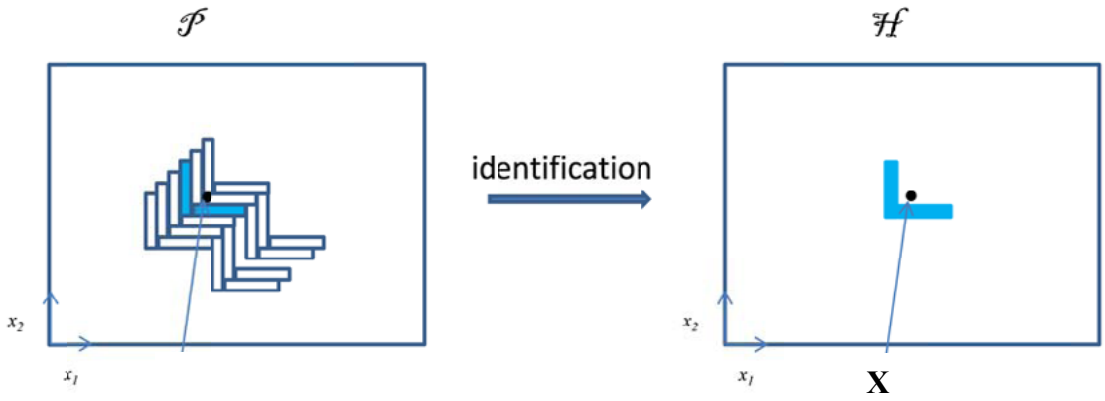

Figure 2: Identification between REV and a 2D continuum.

Analogously to what done for the discrete model, the kinematic descriptors of a generic point belonging to the 2D continuum are represented by $\dot{\mathbf{w}}(\mathbf{x})$ and $\boldsymbol{\Omega}(\mathbf{x})$ fields, namely the velocity and angular velocity tensors of the point $\mathbf{x}$ respectively.

For a Cauchy continuum, the total internal power dissipated is $\pi = \mathbf{N} \cdot \text{sym}(\text{grad}\,\dot{\mathbf{w}})$. In the paper it is also assumed that $\text{sym}(\text{grad}\,\dot{\mathbf{w}}) = \dot{\mathbf{D}}$, where $\dot{\mathbf{D}}$ is the in-plane membrane strain rate tensor and $\dot{D}_{\alpha\beta} = 1/2\left(w_{\alpha,\beta} + w_{\beta,\alpha}\right)$, with the Greek index α=1,2.

From the above considerations, it is possible to assign a correspondence between a class of regular motions in $\mathcal{P}$ and $\mathcal{H}$. In particular, it is assumed that the velocity and angular velocity of the center of the brick $B_{i,j}$ and $B_{i+\frac{1}{2},j+\frac{1}{2}}$ in the discrete system and the velocity and angular velocity of the center of the REV in the continuum model are the same, i.e.:

$$\dot{\mathbf{w}}^{i,j}(\mathbf{x}) = \dot{\mathbf{w}}(\mathbf{x}) + \text{grad}\,\dot{\mathbf{w}}(\mathbf{x})\left(\mathbf{g}^{i,j} - \mathbf{x}\right) \qquad \boldsymbol{\Omega}^{i,j}(\mathbf{x}) = \boldsymbol{\Omega}(\mathbf{x}) + \text{grad}\,\boldsymbol{\Omega}(\mathbf{x})\left(\mathbf{g}^{i,j} - \mathbf{x}\right) \tag{5}$$

and

$$\dot{\mathbf{w}}^{i+\frac{1}{2},j+\frac{1}{2}}(\mathbf{x}) = \dot{\mathbf{w}}(\mathbf{x}) + \text{grad}\,\dot{\mathbf{w}}(\mathbf{x})\left(\mathbf{g}^{i+\frac{1}{2},j+\frac{1}{2}} - \mathbf{x}\right) \qquad \boldsymbol{\Omega}^{i+\frac{1}{2},j+\frac{1}{2}}(\mathbf{x}) = \boldsymbol{\Omega}(\mathbf{x}) + \text{grad}\,\boldsymbol{\Omega}(\mathbf{x})\left(\mathbf{g}^{i+\frac{1}{2},j+\frac{1}{2}} - \mathbf{x}\right) \tag{6}$$

Where $\mathbf{g}^{i,j}$ and $\mathbf{g}^{i+\frac{1}{2},j+\frac{1}{2}}$ are the centroids of $B_{i,j}$ and $B_{i+\frac{1}{2},j+\frac{1}{2}} \in \mathcal{P}$ generic couple of bricks and a first order Taylor approximation (first order identification) in the velocity and angular velocity is used.

In the discrete system, the contact forces between blocks $B_{i,j}$ and $B_{i+\frac{1}{2},j+\frac{1}{2}}$ are $\mathbf{t}^{i,j}(\xi)$ and $\mathbf{t}^{i+\frac{1}{2},j+\frac{1}{2}}(\xi)$ for $\xi \in$ I, being ξ a generic point on the interface I. Equilibrium condition requires that $\mathbf{t}^{i,j}(\xi) = -\mathbf{t}^{i+\frac{1}{2},j+\frac{1}{2}}(\xi)$. Hence, the power dissipated at the interface is:

$$\pi = \int_I \mathbf{t}(\xi) \cdot \left[\dot{\mathbf{w}}^{i+\frac{1}{2},j+\frac{1}{2}}(\xi) - \dot{\mathbf{w}}^{i,j}(\xi)\right] \tag{7}$$

At this stage, for a chosen REV and a given class of regular motions, it is imposed that the mechanical power dissipated by the contact actions on $\mathcal{P}$ and $\mathcal{H}$ coincides. Under these assumptions, the membrane tensor $\mathbf{N}$ may be expressed as a function of the vector $\mathbf{t}_p$, i.e. as a function of the measure of the stress in the micro-mechanical model.

$$\mathbf{N} = \frac{1}{2\mathrm{A}} \sum_{\mathrm{n}} \mathrm{sym} \mathbf{t}_{\mathrm{p}} \otimes \left(\mathbf{g}^{\mathrm{i}+\frac{1}{2},\mathrm{j}+\frac{1}{2}} - \mathbf{g}^{\mathrm{i,j}} \right) \tag{8}$$

where A is the area of the chosen REV and the symbol $\sum$ indicates a summation extended to all the interfaces to which the chosen REV is in contact.

It is finally interesting to point out that the 1/2 coefficient appearing in the above expression for **N** is relative only to the external interfaces of the REV, because such interfaces are shared by contiguous REVs, while in the case of internal interfaces, the coefficient is equal to 1.

3 LINEAR ELASTIC CASE

After the preliminary characterization of powers expended on the continuum model and the regular assemblage of blocks, the constitutive homogenized functions for masonry may be introduced. In particular, for rigid blocks and linear elastic cohesive interfaces, the $\mathbf{A}^F = \left(A_{\alpha\beta\kappa\delta}\right)^F$ homogenized membrane elastic tensor (corresponding to a prescribed $\dot{\mathbf{D}}$ macroscopic strain field rate) may be defined as follows:

$$\overline{\mathbf{N}} = t < \overline{\boldsymbol{\sigma}} >_Y = \mathbf{A}^F \dot{\mathbf{D}} \tag{9}$$

Where $< \cdot >_Y$ is the average operator defined in Y and $\overline{\mathbf{N}} = \left(N_{\alpha\beta}\right)$ is the macroscopic in-plane (membranal) actions field for the homogenized material.

If blocks are assumed as rigid bodies and mortar joint is reduced to an interface with linear elastic behavior, the interaction between a generic couple of $B_{i,j}$ and $B_{i+\frac{1}{2},j+\frac{1}{2}}$ blocks may be defined by the constitutive elastic tensor $\mathbf{K}$ between the $\mathbf{t}$ tractions at the I interface and the $[\mathbf{w}]$ jump of displacement field at the I, as:

$$\mathrm{K}_{ij} = \frac{1}{e} \mathrm{a}^M_{iklj} n_k n_l \tag{10}$$

Here e is the actual thickness of the joint, $\mathbf{a}^M$ is the mortar constitutive functions and $\mathbf{n}$ is the normal to the interface. In the isotropic case, the above expression becomes:

$$\mathbf{K} = \frac{1}{e} \left(\mu^M \mathbf{I} + \left(\mu^M + \lambda^M \right) (\mathbf{n} \otimes \mathbf{n}) \right) \tag{11}$$

where μ^M and λ^M are the Lamé constants of the mortar and $\mathbf{I}$ is the identity tensor, see [11]. (11) may be easily re-written as a function of E^M and ν^M mortar Young and Poisson ratio as follows:

$$\mathbf{K} = \frac{1}{e} \left[\frac{\mathrm{E}^M}{2(1+\nu^M)} \left(\mathbf{I} + \frac{1}{(1-2\nu^M)} (\mathbf{n} \otimes \mathbf{n}) \right) \right] \tag{12}$$

It is interesting to notice that the **K** tensor has, in this case, a diagonal form and that, in linear elasticity, the formulation is substituted with a work-based approach, assuming displacements instead of velocities as kinematic variables.

In analogy to what done previously in the general case, the field problem may be defined on the Y characteristic module. It must be noted that the field problem is written exclusively as a function of the block size.

The internal work of the interfaces formally is identical to the power relation written in the general case and becomes:

$$\pi^{k1,k2} = \int_I \mathbf{t}(\xi) \cdot \left[\mathbf{w}^{i+\frac{1}{2},j+\frac{1}{2}}(\xi) - \mathbf{w}^{i,j}(\xi) \right] = \int_I \left[\mathbf{w}^{i+\frac{1}{2},j+\frac{1}{2}}(\xi) - \mathbf{w}^{i,j}(\xi) \right]^T \mathbf{K} \left[\mathbf{w}^{i+\frac{1}{2},j+\frac{1}{2}}(\xi) - \mathbf{w}^{i,j}(\xi) \right] \quad (13)$$

By minimizing the internal work expressed in (13) by means of a standard quadratic programming routine, the constitutive functions $\mathbf{A}^F = \left(A_{\alpha\beta\kappa\delta}\right)^F$ representing the homogenized membrane elastic tensor may be evaluated numerically.

In the numerical simulations, standard Italian UNI bricks of dimensions 55 mm × 12 mm × 250 mm (height × thickness × length) are assumed.

In Figure 3, the trends of the homogenized $\mathbf{A}^F = \left(A_{\alpha\beta\kappa\delta}\right)^F$ membrane moduli are represented varying the E^M/E^B ratio, when the E^B Young modulus of the block is assumed equal to 10000 MPa and E^M varies from 1000 to 5000 MPa. Poisson ratios of both mortar and block (ν^M and ν^B respectively) are assumed identically equal to 0.2. As can be noted, the sensitivity of the results to mortar thickness decreases considerably when E^M/E^B increases, and, as expected, the difference tends to vanish for E^M/E^B =1 (homogeneous case).

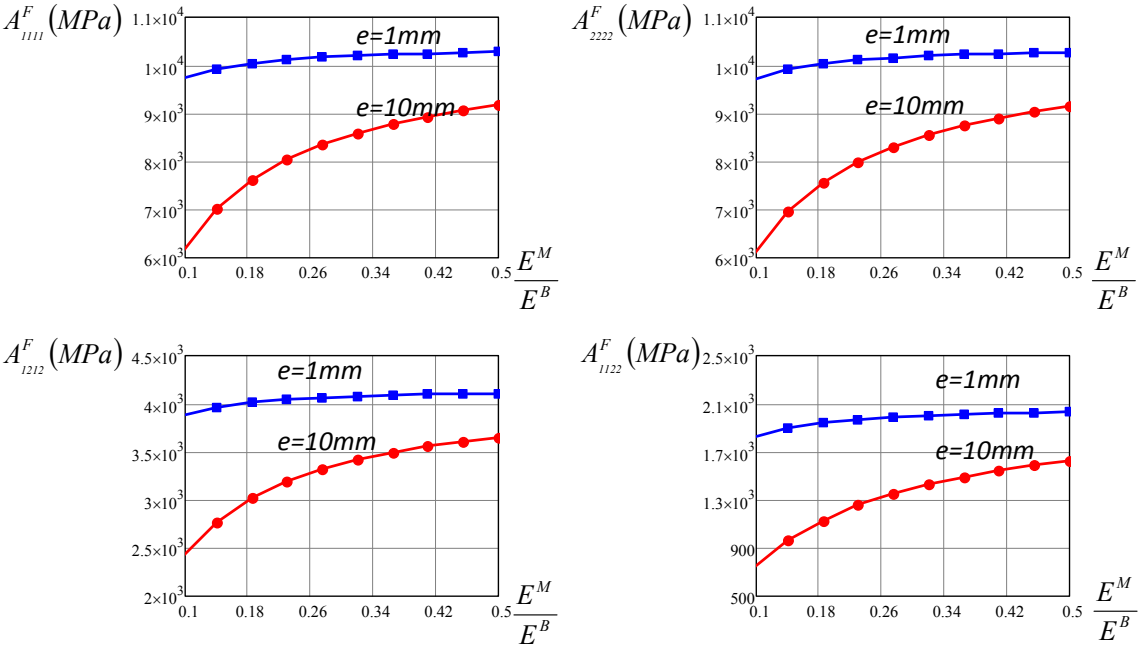

Figure 3: Trends of the homogenized $\mathbf{A}^F = \left(A_{\alpha\beta\kappa\delta}\right)^F$ membrane moduli as a function of E^M/E^B ratio and with different thicknesses for the mortar joint.

4 HOMOGENIZED FAILURE SURFACES

A Mohr-Coulomb failure criterion with tension cut-off f_t and a linearized cap in compression (f_c, Φ_2), see [5], is assumed for joints. A classic Mohr-Coulomb failure criterion may be obtained as particular case when $f_t = c/\tan\Phi$ and $f_c \to \infty$.

A piecewise linear approximation of the failure surface $G = G(\boldsymbol{\sigma})$ is adopted for each interface I of area A^I, constituted by n_{lin} planes of equation $\mathbf{A}_i^{I\,T}\boldsymbol{\sigma} = c_i^I \quad 1 \le i \le n_{lin}$, where $\boldsymbol{\sigma} = [\sigma_{22} \quad \sigma_{21} \quad \sigma_{23}]$, σ_{22} is the normal stress on the interface and σ_{21} and σ_{23} are tangential stresses along two assigned perpendicular directions, see [9][10] for a detailed description of the numerical model.

$3 \cdot n_{lin}$ independent plastic multiplier rates have to be assumed as optimization variables for each interface, dealing with a simple set of 3 linear equations involving plastic multiplier rates fields $\dot{\lambda}_i^I(\xi_1, \xi_3)$ and velocity jump $[\dot{\mathbf{w}}(\xi_1, \xi_3)]$ in each point $\boldsymbol{\xi} = [\xi_1 \quad \xi_3] \in I$:

$$[\dot{\mathbf{w}}(\xi_1, \xi_3)] = \sum_{i=1}^{n_{lin}} \dot{\lambda}_i^I(\xi_1, \xi_3) \frac{\partial G}{\partial \boldsymbol{\sigma}} \tag{14}$$

In equation (14), we assume that $[\dot{\mathbf{w}}(\xi_1, \xi_3)] = [\Delta\dot{w}_2 \quad \Delta\dot{w}_1 \quad \Delta\dot{w}_3]^T$ is the jump of velocity field (linear in (ξ_1, ξ_3)) on the I-th interface and $\Delta\dot{w}_j$ corresponds to the jump along the direction j, whereas $\dot{\lambda}_i^I(\xi_1, \xi_3)$ is the i-th plastic multiplier rate field (linear in (ξ_1, ξ_3)) of the interface I, associated to the i-th linearization plane of the failure surface. In order to satisfy equation (14) for each point of the interface I, nine equality constraints for each interface have to be imposed.

Internal power dissipation occurs only on interfaces. For a generic I-th interface, such dissipation is defined as the product of the interface stress vector for the jump of velocities field, i.e. from equation (14):

$$\pi_{\text{int}}^I = \int_{A^I} [\dot{\mathbf{w}}]^T \boldsymbol{\sigma} dA^I = \int_{A^I} \sum_{i=1}^{n_{lin}} \dot{\lambda}_i^I(\xi_1, \xi_3) \left[\frac{\partial G}{\partial \boldsymbol{\sigma}}\right]^T \boldsymbol{\sigma} dA^I = \frac{1}{3} \sum_{i=1}^{n_{lin}} c_i^I \sum_{k=1}^{3} \dot{\lambda}_i^I(\xi_1^k, \xi_3^k) A^I \tag{15}$$

where c_i^I is the right hand side of the i-th linearization plane of the interface I failure surface.

External power is evaluated applying the macroscopic deformation tensor $\dot{\mathbf{D}}$, which is hereafter re-arranged in a 3x1 vector $\tilde{\dot{\mathbf{D}}}$ (where shear contribution $\tilde{\dot{D}}_3 = \frac{1}{2}(D_{12} + D_{21})$) to facilitate numerical computations.

In the in-plane case, external power dissipated can be written as $\pi_{ext} = (\boldsymbol{\Sigma}_0^T + \lambda \boldsymbol{\Sigma}_1^T)\tilde{\dot{\mathbf{D}}}$, where $\boldsymbol{\Sigma}_0$ is the vector of permanent loads, λ is the load multiplier, $\boldsymbol{\Sigma}_1^T$ is the vector of loads dependent on the load multiplier. As the amplitude of the failure mechanism is arbitrary, a

further normalization condition $\boldsymbol{\Sigma}_1^T \tilde{\dot{\mathbf{D}}} = 1$ is usually introduced. Hence, the external power becomes linear in $\tilde{\dot{\mathbf{D}}}$.

After a series of algebraic passages not reported here for the sake of conciseness, the following linear programming problem is obtained:

$$\begin{cases} \min\{\lambda\} = \sum_{I=1}^{n^I} \pi_{\text{int}}^I - \boldsymbol{\Sigma}_0^T \tilde{\dot{\mathbf{D}}} \\ \mathbf{n}_{\boldsymbol{\Sigma}}{}^T \tilde{\dot{\mathbf{D}}} = 1 \quad \mathbf{n}_{\boldsymbol{\Sigma}}{}^T \mathbf{n}_k = 0 \ \forall k \neq i, j \\ \mathbf{G}^I(\boldsymbol{\xi}_k) \tilde{\dot{\mathbf{D}}} = [\mathbf{w}(\boldsymbol{\xi}_k)] = \sum_{i=1}^{n_{lin}} \dot{\lambda}_i^I(\xi_1^k, \xi_3^k) \dfrac{\partial G}{\partial \boldsymbol{\sigma}} \end{cases} \quad (16)$$

Where:

- λ represents the collapse load when a direction $\mathbf{n}_{\boldsymbol{\Sigma}}$ in the $\boldsymbol{\Sigma}$ space is assigned;
- $\mathbf{n}_k$ is a versor such that $\Sigma_k = \boldsymbol{\Sigma}^T \mathbf{n}_k$;
- i and j represent the axes of projection of G_p^{hom}.

When dealing with the numerical simulations, standard Italian UNI bricks of dimensions 5.5 cm × 12 cm × 25 cm (height × thickness × length) and mortar joints reduced to interfaces obeying a linearized Lourenço & Rots [5] failure criterion are considered. Mechanical properties adopted for the joints are the following: tensile strength f_t 0.1 MPa, cohesion $c = f_t$, friction angle Φ=36°, compression strength f_c=3.5 MPa, shape of the linearized compression cap Φ_2=30°.

The results of the limit analyses are summarized from Figure 4 to Figure 6.

In particular, in Figure 4-a, strength domain sections in the tension-tension region obtained by the homogenization approach are depicted. Three different orientations (0°, 22.5° and 45°) of the principal stress directions (Σ_{11}) with respect to horizontal axis are plotted. Results may be directly compared with those relevant for a running bond pattern, reported in Figure 4-b, where exactly the same mechanical properties for the joints and the same brick geometry have been assumed.

As it is possible to notice, the differences induced by the utilization of different patterns are rather marked, especially when dealing with the orthotropy ratio along horizontal and vertical direction. The differences between the two patterns are quite evident, with an extra-resistance provided by herringbone bond in vertical direction equal to 1.8. The same comparisons are replicated in Figure 5 and Figure 6 in the compression-tension and compression-compression region respectively. From an overall analysis of strength domain sections, it appears that globally (the term is intended as along the majority of the directions), the strength exhibited by herringbone bond may be rather higher than that provided by a running bond disposition of the bricks. Especially in the compression-tension region, the difference appears drastic.

Finally, the examples discussed underline that masonry macroscopic failure surface results dependent both on the geometrical and mechanical characteristics assumed for the components and that the proposed model may be able to reproduce different macroscopic strength domains whenever different failure behaviors for the components are taken into account.

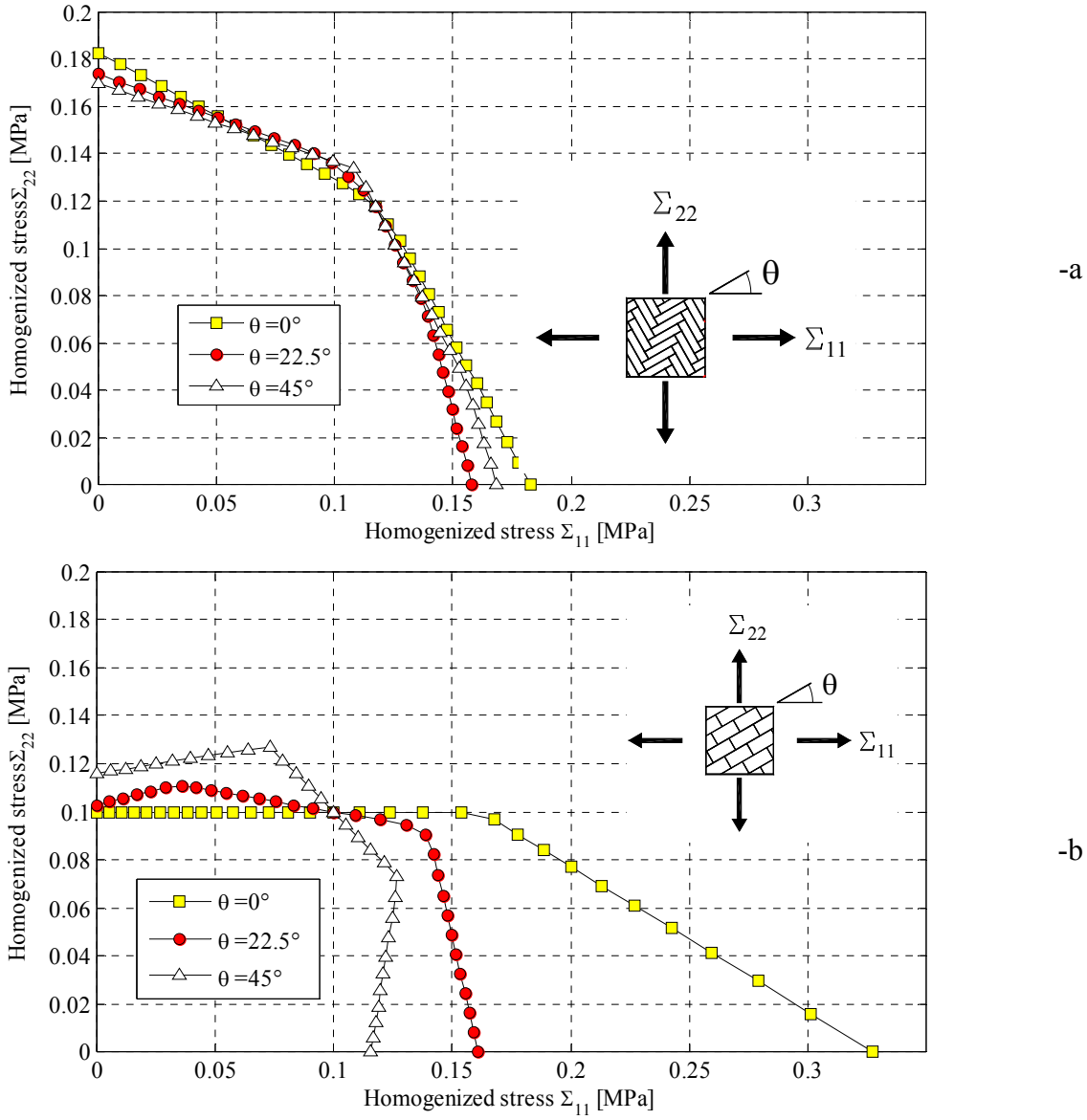

Figure 4: In-plane failure surfaces at different orientation of principal axes with respect to horizontal direction, tension-tension region. –a: herringbone bond. –b: running bond.

4 CONCLUSIONS

A kinematic procedure for the determination of (1) the in-plane homogenized elastic moduli and (2) the macroscopic strength domains for herringbone masonry, has been proposed. The procedure relies into the identification of a REV constituted by two central bricks interacting with their neighbors by means of either elastic or rigid-plastic interfaces with friction, representing mortar joints. A sub-class of possible elementary deformations has been a-priori chosen to describe joints cracking under in-plane loads and the "identification"

of the discrete model has been obtained equating power expended within the 3D bricks assemblage to that dissipated in the macroscopic 2D Cauchy continuum. The elastic and limit analysis problem at a cell level have been solved respectively through a quadratic and linear programming approach.

When dealing with the limit analysis approach, the roles played by (1) the direction of the load with respect to herringbone bond inclination and (2) masonry texture have been investigated.

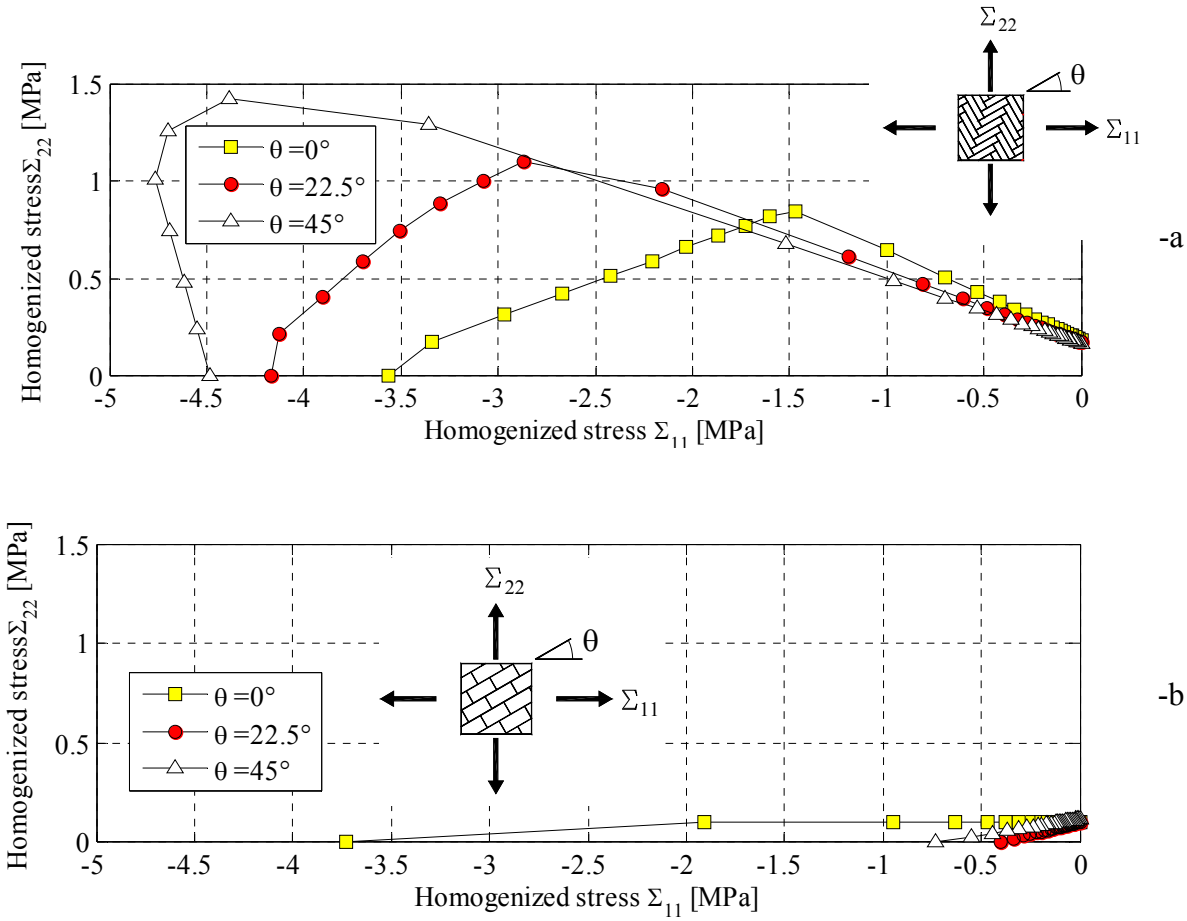

Figure 5: In-plane failure surfaces at different orientation of principal axes with respect to horizontal direction, compression-tension region. –a: herringbone bond. –b: running bond.

REFERENCES

[1] Luciano, R., and Sacco, E. Homogenization technique and damage model for old masonry material. *International Journal of Solids and Structures* (1997) **34**(24): 3191-3208.

[2] Massart, T.J., Peerlings, R.H.J., and Geers, M.G.D. An enhanced multi-scale approach for masonry wall computations with localization of damage. *International Journal for Numerical Methods in Engineering* (2007) **69**(5): 1022-1059.

[3] Milani, G. Simple homogenization model for the non-linear analysis of in-plane loaded masonry walls. *Computers & Structures* (2011) **89**: 1586–1601.

[4] Milani, G., Lourenço, P.B., and Tralli, A. Homogenised limit analysis of masonry walls. Part I: failure surfaces. *Computers and Structures* (2006) **84**(3-4): 181-195.
[5] Lourenço, P.B., and Rots, J. A multi-surface interface model for the analysis of masonry structures. *Journal of Engineering Mechanics ASCE* (1997) **123**(7): 660-668.
[6] Milani, G. 3D upper bound limit analysis of multi-leaf masonry walls. *International Journal of Mechanical Sciences* (2008) **50**(4): 817-836.
[7] Milani, G., Zuccarello, F.A., Olivito, R.S., Tralli, A. Heterogeneous upper-bound finite element limit analysis of masonry walls out-of-plane loaded. *Computational Mechanics* (2007) **40**(6): 911-931.
[8] Bacigalupo, A., Cavicchi, A., and Gambarotta, L. A simplified evaluation of the influence of the bond pattern on the brickwork limit strength. *Advanced Materials Research* (2012) **368-373**: 3495-3508.
[9] Cecchi, A., Milani, G., and Tralli, A A Reissner-Mindlin limit analysis model for out-of-plane loaded running bond masonry walls. *International Journal of Solids and Structures* (2007) **44**(5): 1438-1460.
[10] Cecchi, A., and Milani, G. A kinematic FE limit analysis model for thick English bond masonry walls. *International Journal of Solids and Structures* (2008) **45**: 1302–1331.
[11] Klarbring, A. Derivation of model of adhesively bounded joints by the asymptotic expansion method. *Int J Eng Sci* (1991) **29**: 493-512.

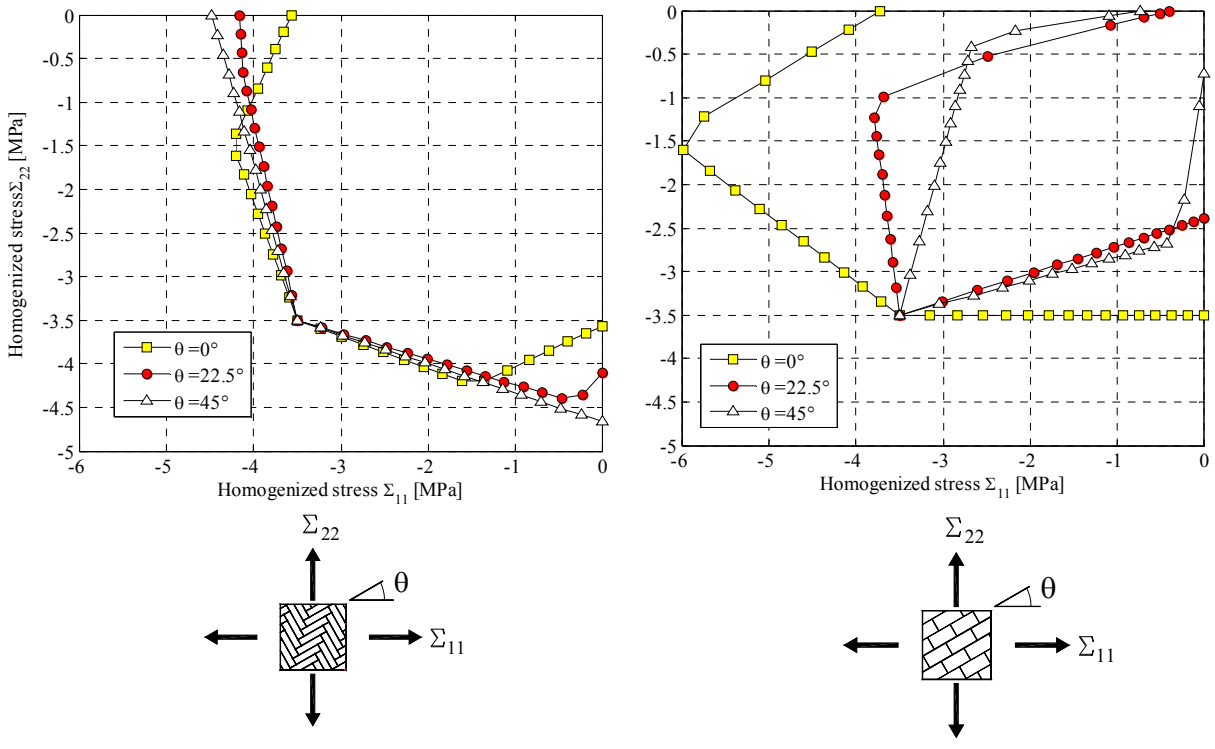

Figure 6: In-plane failure surfaces at different orientation of principal axes with respect to horizontal direction, compression-compression region. –a: herringbone bond. –b: running bond.